



# Development of a New Electrochemical Sensor Based on Mag-MIP Selective Toward Amoxicillin in Different Samples

Rosario López<sup>1</sup>, Sabir Khan<sup>1,2</sup>, Ademar Wong<sup>2,3</sup>, María del Pilar Taboada Sotomayor<sup>2,3\*</sup> and Gino Picasso<sup>1\*</sup>

<sup>1</sup> Laboratory of Physical Chemistry Research, Faculty of Sciences, National University of Engineering, Lima, Peru, <sup>2</sup> Analytical Department, Chemistry Institute, State University of São Paulo (UNESP), Araraquara, Brazil, <sup>3</sup> National Institute for Alternative Technologies of Detection, Toxicological Evaluation & Removal of Micropollutants and Radioactives (INCT-DATREM), Araraquara, Brazil

## OPEN ACCESS

### Edited by:

Karin Chumbimuni-Torres,  
University of Central Florida,  
United States

### Reviewed by:

Hassan Karimi-maleh,  
University of Electronic Science and  
Technology of China, China  
Pramod K. Kalambate,  
Huazhong University of Science and  
Technology, China

### \*Correspondence:

María del Pilar Taboada Sotomayor  
m.sotomayor@unesp.br;  
mpilarts@hotmail.com  
Gino Picasso  
gpicasso@uni.edu.pe

### Specialty section:

This article was submitted to  
Analytical Chemistry,  
a section of the journal  
Frontiers in Chemistry

**Received:** 09 October 2020

**Accepted:** 22 February 2021

**Published:** 19 March 2021

### Citation:

López R, Khan S, Wong A,  
Sotomayor MDPT and Picasso G  
(2021) Development of a New  
Electrochemical Sensor Based on  
Mag-MIP Selective Toward Amoxicillin  
in Different Samples.  
*Front. Chem.* 9:615602.  
doi: 10.3389/fchem.2021.615602

This work describes an electrochemical sensor for the selective recognition and quantification of amoxicillin and a  $\beta$ -lactam antibiotic in real samples. This sensor consists of a carbon paste electrode (CPE) modified with mag-MIP (magnetic molecularly imprinted polymer), which was prepared by precipitation method via free radical using acrylamide (AAm) as functional monomer, N,N'-methylenebisacrylamide (MBAA) as a crosslinker, and potassium persulfate (KPS) as initiator, to functionalized magnetic nanoparticles. The magnetic non-imprinted polymers (mag-NIP) were prepared using the same experimental procedure without analyte and used for the preparation of a CPE for comparative studies. The morphological, structural, and electrochemical characteristics of the nanostructured material were evaluated using Field emission gun scanning electron microscopy (FEG-SEM), Transmission electron microscopy (TEM), Fourier transform infrared spectroscopy (FTIR), Vibrating sample magnetometry (VSM), X-ray diffraction (XRD), and voltammetric technique. Electrochemical experiments performed by square wave voltammetry show that the mag-MIP/CPE sensor had a better signal response compared to the non-imprinted polymer-modified electrode (mag-NIP/CPE). The sensor showed a linear range from 2.5 to 57  $\mu\text{mol L}^{-1}$  of amoxicillin ( $r^2 = 0.9964$ ), with a limit of detection and a limit of quantification of 0.75 and 2.48  $\mu\text{mol L}^{-1}$ , respectively. No significant interference in the electrochemical signal of amoxicillin was observed during the testing experiments in real samples (skimmed milk and river water). The proposed mag-MIP/CPE sensor could be used as a good alternative method to confront other techniques to determine amoxicillin in different samples.

**Keywords:** mag-MIP, amoxicillin, electrochemical sensor, selective adsorption, carbon paste electrode

## INTRODUCTION

Pharmaceuticals are used domestically in veterinary medicine and hospitals, and could be analgesics, antibiotics, anti-inflammatory, antiepileptic, antidepressants, hormones, statins, beta-blockers, and products of contrasts, among others (Miège et al., 2009). Drugs that have been administered to a large extent in humans or animals are largely excreted directly through the urine

(unmetabolized 55–80%) and feces and other parts of the body (Verlicchi et al., 2010) that persist in the environment. Among pharmaceuticals, antibiotics are the most widely used in the treatment of bacterial infections, for improving health in humans, for preventing and treating animals and plant infections, and promoting growth in animal farming (Martinez, 2009).

Antibiotics can reach the environment by various means, such as excretion in urine and feces, direct disposal of unused or expired drugs by drug factories, hospitals, and veterinary surgeries (Christou et al., 2017). The presence of antibiotics in the environment, for example in natural water and soil, principally causes antibiotic resistance, hypersensitivity reaction, and aplastic anemia in sensitive humans. Antibiotic resistance is an adaptative genetic natural phenomenon possessed or acquired by bacteria in which it can grow and survive, even when in the presence of an antibiotic of therapeutic concentration. In this way, multiple-antibiotic-resistant pathogenic bacteria exist in the environment, known as superbugs (Carvalho and Santos, 2016). The World Health Organization (WHO) outlines that at least 700,000 people die each year due to drug-resistant diseases. Of these, ~230,000 people die from multidrug-resistant tuberculosis, as well as common diseases, including respiratory tract infections, sexually transmitted infections, and urinary tract infections, which are untreatable (World Health Organization, 2019).

Amoxicillin is a  $\beta$ -lactam antibiotic semi-synthetic widely used in human and veterinary medicine for the treatment of infections since it has a wide spectrum of action in gram-positive and gram-negative bacteria. For this reason, amoxicillin is used as the first-line antibiotic in different countries around the world, including Italy, the UK, Australia, Brazil, and Korea, which have the highest sales (World Health Organization, 2019). Globally, amoxicillin is one of the most used and prescribed antibiotics, especially in the public sector for the treatment of colds, pharyngitis, and bronchospasms. It can be acquired relatively easily without a medical prescription in various countries (Ecker et al., 2013). In human medicine, it is used for the treatment and prevention of respiratory, gastrointestinal, urinary, and skin bacterial infections. In animal medicine, amoxicillin is also used for the treatment and prevention of disease and to promote the growth of domestic (dogs, cats) and food animals (livestock, horses, pigs, goats, sheep, etc.) (Elizalde-Velázquez et al., 2016). The time it takes for the concentration of the amoxicillin in the plasma or the total amount in the body to be reduced by 50% is 1–1.5 h (terminal half-life of elimination), the excretion is renal and almost 80% of the unmetabolized amoxicillin is mainly excreted in the urine but is also secreted in milk. For these reasons, a wide range of concentrations, from traces to high levels, of this drug are found in surface water or wastewater.

Various analytical methods have been reported for the determination of amoxicillin such as HPLC (Pires de Abreu et al., 2003), spectrophotometric (Kishore et al., 2011), capillary electrophoresis (Hancu et al., 2016) as well as electrochemical methods (Fouladgar et al., 2011). The electrochemical sensor is a promising technology due to its simplicity and diversity. Moreover, the method has high repeatability, a good sensitivity,

a low cost and is environmental friendly compared to the other analytical methods used for different types of analytes as drugs and food (Karimi-Maleh et al., 2016, 2020a,b; Karimi-Maleh and Arotiba, 2020).

In the present study, a mag-MIP with recognition sites for amoxicillin was synthesized, and this polymer was then used as a modifier in the carbon paste electrode for the detection of amoxicillin in milk and river water samples. Mag-MIP are materials based on magnetic nanoparticles (mag) coated with a molecularly imprinted polymer (MIP) that have attracted much attention due to their high magnetic character, chemical stability, ease of preparation, and low cost. The material has advantages such as a good sensibility, a high surface area, durability, and reusability as well as high selectivity toward amoxicillin.

## MATERIALS AND METHODS

### Reagents and Solutions

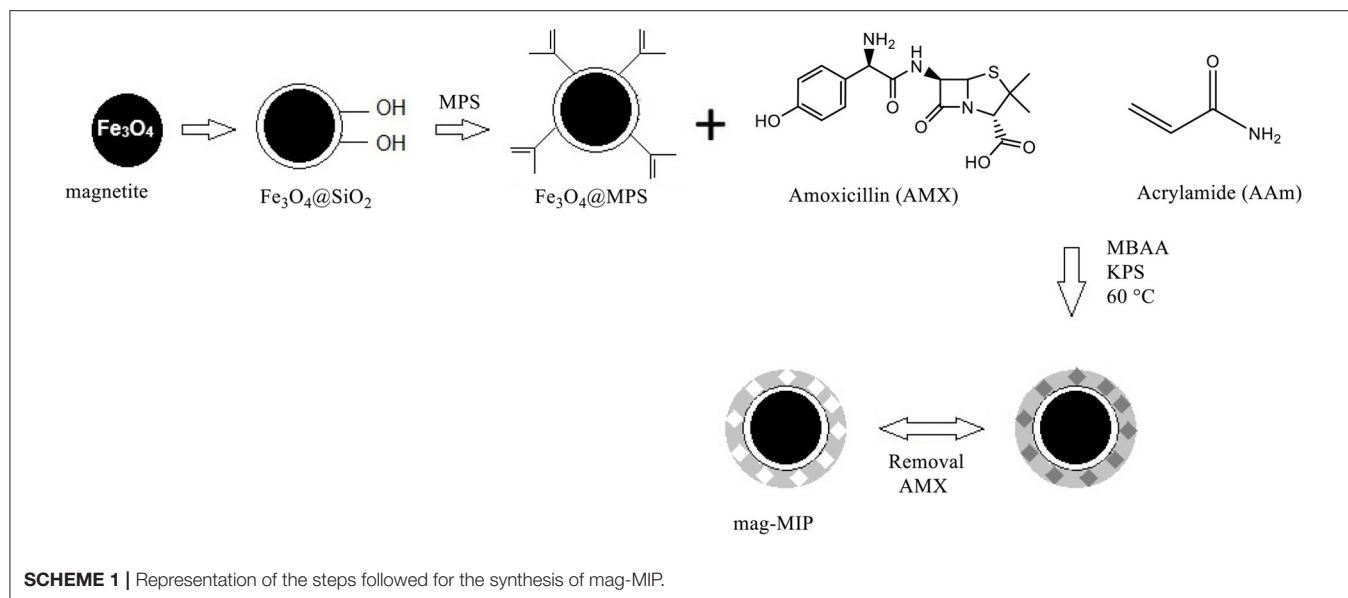
All the reagents used in this work were of analytical grade. All solutions were prepared in ultrapure water (18 M $\Omega$  at 25°C) obtained from Milli-Q Direct-0.3 (Millipore). Ethyl acetate, triethyleneglycol (TREG), acetylacetonate [Fe(acac)<sub>3</sub>, 97%], ethanol absolute, ammonia solution (23–28% v/v), anhydrous toluene, tetraethyl orthosilicate (TEOS), and methanol (HPLC grade), sodium phosphate (monobasic and dibasic) purchased from Merck. Meanwhile, 3-methylpropyltrimethoxysilane (MPS), acrylamide (AAM), amoxicillin, potassium persulfate (KPS), *N*, *N'*-methylenebisacrylamide (MBAA), graphite, and mineral oil were acquired from Sigma–Aldrich. Ultrapure water (UP, 18.2 M $\Omega$  cm at 298 K) was used for all the experiments and was obtained from a Purelab Classic water purification system. The stock solution of amoxicillin (10  $\mu$ mol L<sup>-1</sup>) was prepared in 0.1 mol L<sup>-1</sup> sodium hydroxide solution.

### Mag-MIP and Mag-NIP Particles Synthesis

Magnetite nanoparticles were prepared following the polyol method (Cai and Wan, 2007; Vega-Chacón et al., 2016). Fe(acac)<sub>3</sub> was dissolved in TREG using a mechanical stirrer in a three-necked round-bottomed flask equipped with a condenser and nitrogen gas which was passed through the reaction solution. The mixture was heated at 120°C for 30 min, then at 180°C for 30 min, and finally at 280°C for 60 min. The suspension was then cooled to room temperature.

A solution of ethanol and ethyl acetate (1:6) was added to the suspension. The nanoparticles were separated from the solution by magnetic-field-assisted sedimentation procedure employing a neodymium magnet and the supernatant was discarded. The nanoparticles were subsequently suspended in an ethanol-ethyl acetate solution. The magnetic separation and suspension processes were repeated until the supernatant was colorless. The nanoparticles were then dried at 50°C. The surface of the Fe<sub>3</sub>O<sub>4</sub> nanoparticles was covered by silica through the Stöber sol-gel method (Stöber et al., 1968).

A quantity of 300 mg Fe<sub>3</sub>O<sub>4</sub> nanoparticles was dispersed in 44 mL water-ethanol solution (1:10) using a sonicator. Then, 5 mL of ammonium hydroxide 28% (v/v) was added to the suspension, and immediately 2 mL of TEOS was added dropwise



under continuous stirring and nitrogen gas flow. The reaction was allowed to proceed for 12 h at room temperature.

The obtained nanoparticles were separated by magnetic-field-assisted sedimentation, washed with water several times, and later were dried at 50°C. To introduce methacrylate groups on the surface, Fe<sub>3</sub>O<sub>4</sub>@SiO<sub>2</sub> nanoparticles were functionalized with MPS. Fe<sub>3</sub>O<sub>4</sub>@SiO<sub>2</sub> nanoparticles (250 mg) were sonically dispersed in 50 mL of dried toluene. Subsequently, 5 mL of MPS was added to the organic dispersion under continuous stirring and nitrogen gas flow. The reaction was allowed to proceed for 12 h at room temperature. The nanoparticles were then magnetically separated from the solution, washed with absolute ethanol several times, and dried at room temperature (Khan et al., 2018).

For the synthesis of mag-MIP, a mix of 1 mmol of amoxicillin (analyte) and 4 mmol of AAm (functional monomer) was dissolved in 80 mL of ultrapure water and the solution was stirred for 2 h. Promptly, a quantity of 300 mg of Fe<sub>3</sub>O<sub>4</sub>@SiO<sub>2</sub>-MPS was sonically dispersed and the suspension was stirred for 3 h under continuous stirring and nitrogen gas flow. Then, 100 mmol of MBAA (crosslinker) was added to the suspension and nitrogen gas was bubbled for 10 min. Afterward, 0.185 mmol of KPS (radical initiator) was added to the suspension and the reaction was allowed to progress for 3 h at 60°C. The mag-MIP was separated by vacuum filtration, washed many times with absolute ethanol, and dried at room temperature. The amoxicillin templates were removed using an extraction system (Soxhlet) with solutions of methanol/water (90:10) and methanol/water (70:30), v/v for a period of 8 h. The washing was repeated until no presence of analyte was verified by HPLC during the washing process.

The mag-NIP was prepared in the same way but without the addition of amoxicillin. A schematic representation of all the steps is provided in **Scheme 1**.

## Characterization of Mag-MIP and Mag-NIP

The scanning electron microscopy (SEM) model: (JSM-7500F microscope) was used to characterize the surface morphology of synthesized nanomaterials.

A high-resolution Transmission electron microscope (Model: CM200 super twin with a resolution of 1.9 Å. Company: Philips) was used to evaluate the mag-MIP and mag-NIP particles.

To elucidate the crystalline phase we conducted X-ray diffractometry (XRD) using a Bruker D2 Phaser using Cu K $\alpha$  ( $\lambda = 1.5418 \text{ \AA}$ ) radiation source with a scanning window of 20–90° at 0.4°/s. FTIR spectra were obtained using a Shimadzu FTIR-8400S Prestige-21 spectrophotometer, with the sample in a matrix of KBr to show the functionalization and polymerization through the presence of the different functional groups. Magnetic properties were analyzed by measurements of vibrating sample magnetometry (VSM). The equipment was built for research (Jordán et al., 2018). It shows a hysteresis plot for a magnetic field up to 2,500 Oe with a resolution of  $\sim 2 \times 10^{-4}$  emu.

## Preparation of Mag-MIP/CPE Sensor

The Mag-MIP/CPE sensor was prepared as described in previous works (Wong et al., 2015; Pizan-Aquino et al., 2020) using a mixture of 85 mg of graphite, 15 mg of mag-MIP (or mag-NIP), and 1.0 mL of deionized water. The mixture was carefully homogenized for 20 min, employing a mortar and pestle, and kept for 12 h at room temperature to become dehydrated. Afterward, 80  $\mu$ L of mineral oil was added dropwise, to obtain each modified paste (Khan et al., 2019).

The prepared working paste was used to fill the empty hole of the Teflon<sup>®</sup> working electrode (WE) where a Pt disk was used to provide the electrical connection. The prepared modified electrodes were nominated as mag-MIP/CPE, mag-NIP/CPE, and CPE (carbon paste electrode), prepared for comparison reasons.

## Optimizing the Mag-MIP/CPE Sensor

Electrochemical characterization of amoxicillin was carried out using square wave voltammetry (SWV), in a potentiostat (Model  $\mu$ Autolab Type III, Autolab/Eco Chemie) and with a three-electrode system: mag-MIP/CPE sensor as the working electrode (WE), a commercial Ag/AgCl ( $\text{KCl}_{\text{sat}}$ ) as the reference electrode (RE, Analion<sup>®</sup>) and a platinum wire as the counter electrode (CE).

The effect of potential step increments was studied over the range from 1 to 10 mV, the amplitude was varied over a range from 25 to 100 mV and the frequency was modulated between 8 and 30 Hz with a fixed scan rate of  $10 \text{ mV s}^{-1}$ . Additionally, to explore the mechanism of amoxicillin oxidation on the mag-MIP/CPE sensor, some SWV experiments were made at different pH values ranging from 5.0 to 9.0 in a phosphate buffer solution with a concentration of  $1.0 \text{ mmol L}^{-1}$  to obtain the dependence of the electrochemical oxidation of amoxicillin on pH.

## Application of the Mag-MIP/CPE Sensor to Real Samples

The performance of the mag-MIP/CPE sensor was evaluated by testing river water and milk samples. To this aim, some river water samples were collected from the Gregorio river located in the municipality of São Carlos at the São Paulo State in Brazil. No pre-treatment processes were applied in the samples. The samples were placed in 5 mL capacity flasks and spiked with a standard solution of amoxicillin at three concentration levels. For this,  $400 \mu\text{L}$  of each sample were diluted in  $0.1 \text{ mol L}^{-1}$  phosphate buffer solution (pH 7.0) and analyzed in the electrochemical system with a capacity of 10 mL.

The milk sample was purchased from a supermarket in the same city. The samples were spiked with a standard solution of amoxicillin at 2.5 and  $57 \mu\text{mol L}^{-1}$  concentration level and analyzed in the electrochemical system (at concentrations corresponding in the cell of  $3.0 \times 10^{-6}$  and  $3.0 \times 10^{-5} \text{ mol L}^{-1}$ ). The samples were submitted to the centrifugation process and the supernatant was used in the electrochemical tests.

## RESULT AND DISCUSSION

### Characterization of the Mag-MIP

The SEM and TEM images of the mag-MIP are shown in **Figure 1**, where the morphology and particle size of materials in different stages of synthesis. SEM and TEM micrographs showed the presence of magnetite nanoparticles ( $\text{Fe}_3\text{O}_4$ ) with an average diameter of 10 nm and apparently with a monodisperse distribution (**Figures 1A,B**). In this work, magnetite was successfully synthesized by the polyol method which replaces the traditional and commonly used co-precipitation method for the preparation of superparamagnetic water-soluble nanoparticles, used in various biomedical applications (Cai and Wan, 2007; Vega-Chacón et al., 2016). The SEM and TEM images of silica-coated magnetite nanoparticles are presented in **Figures 1C,D**, respectively. The images indicate that the iron oxide core was coated for an inert silica shell taking a total spherical shape with size up to 300 nm, however, the coated thickness could be varied by changing the amount of TEOS (Laurent et al.,

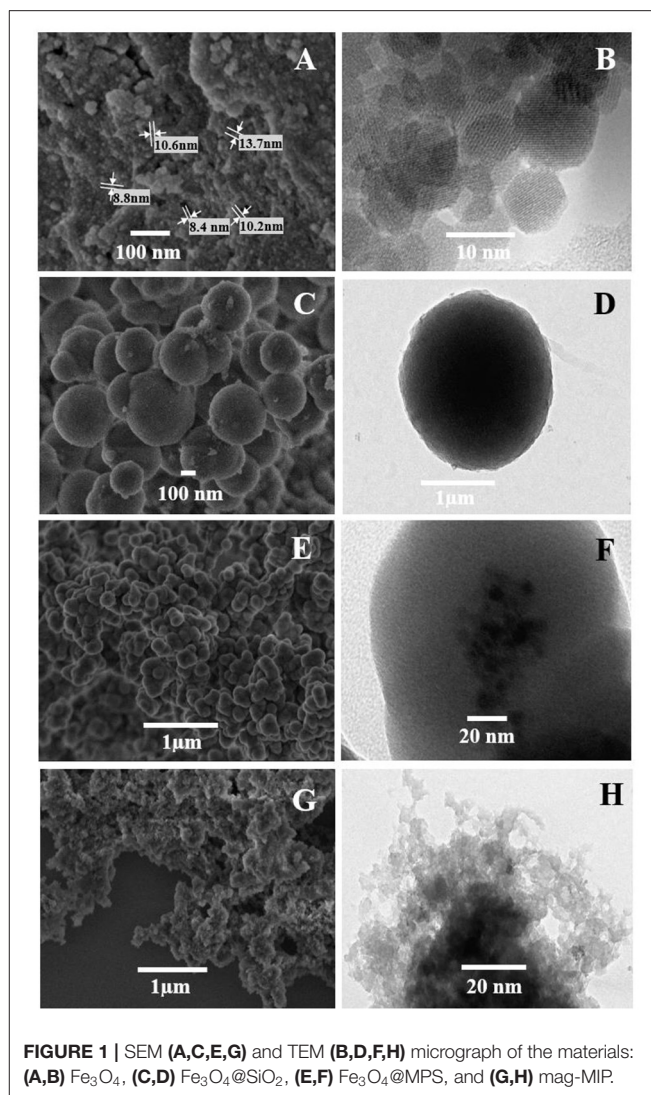
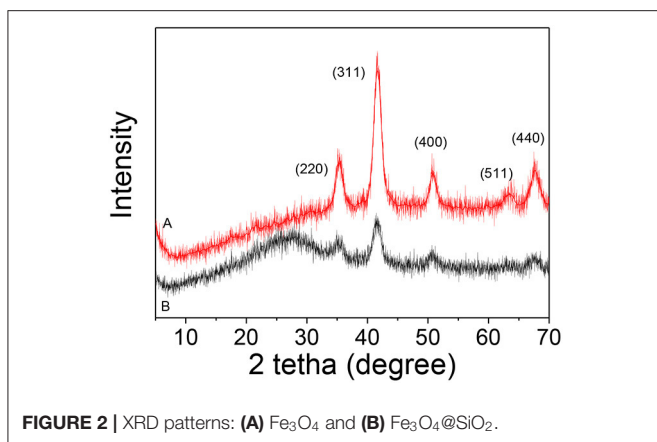


**FIGURE 1** | SEM (A,C,E,G) and TEM (B,D,F,H) micrograph of the materials: (A,B)  $\text{Fe}_3\text{O}_4$ , (C,D)  $\text{Fe}_3\text{O}_4@SiO_2$ , (E,F)  $\text{Fe}_3\text{O}_4@MPS$ , and (G,H) mag-MIP.

2008), modifying the concentration of ammonium and the ratio of tetraethoxysilane (TEOS) to  $\text{H}_2\text{O}$ . The silica shell stabilizes the magnetic nanoparticles and prevents their aggregation in a liquid, as well as improves their chemical stability and provides better protection against toxicity (Lu et al., 2007). An additional covering with MPS is presented in **Figures 1E,F**, which show the spherical-like particles of  $\text{Fe}_3\text{O}_4@SiO_2$ -MPS in which no considerable change in particle size was observed. Here, silanol groups ( $\text{SiOH}$ ) are functionalized by silanes that contain the multiple bonds indispensable for the further polymerization process (Ansari, 2017). Finally, **Figures 1G,H** show the polymerization of the MIP on the agglomerated magnetite nanoparticles (mag-MIP), forming a polymeric layer and full coverage of the magnetic core.

**Figure 2A** shows the XRD pattern of iron oxide nanoparticles synthesized by the polyol method, which observed the highly crystalline cubic spinel structure (JCPDS 19-0629) assigned to magnetite and the high purity of the magnetic nanoparticles

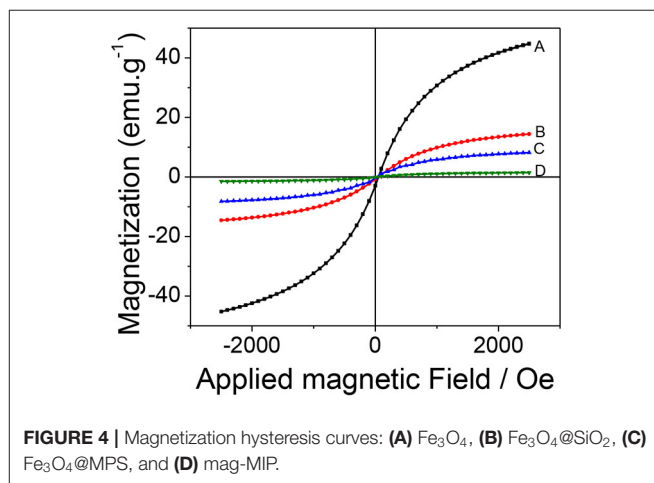
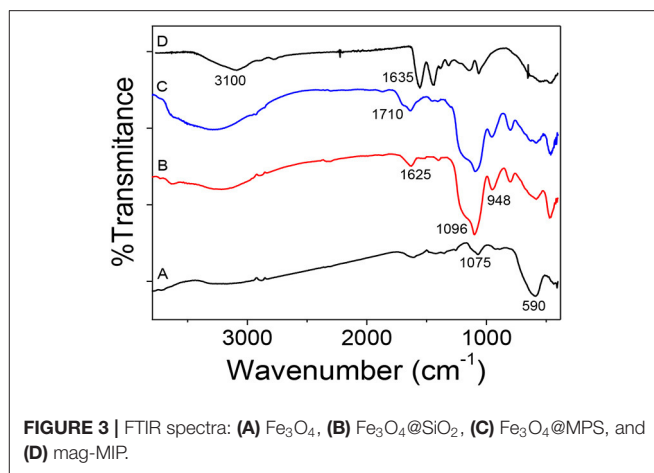




( $\text{Fe}_3\text{O}_4$ ) since no other signal was detected. The silica-coated magnetite ( $\text{Fe}_3\text{O}_4@SiO_2$ ) shows in its diffraction pattern (Figure 2B) an amorphous hump corresponding to the  $SiO_2$  around  $25^\circ$  (Gao et al., 2011) and the rest of the peaks remaining unchanged, from which is inferred that the coating with silica did not affect the starting crystalline structure of the  $\text{Fe}_3\text{O}_4$  (Chang et al., 2012).

Figure 3 shows the FTIR spectra of the evolution from  $\text{Fe}_3\text{O}_4$  to mag-MIP to verify the functional groups that appear during the synthesis. In Figure 3A, the inverse spinel structure of magnetite was again confirmed by IR bands, from the vibrations Fe–O–Fe at  $590$  and  $1,075\text{ cm}^{-1}$  characteristic of vibration of Fe–O stretching at tetrahedral sites. In Figure 3B, for magnetite coated with  $SiO_2$ , some characteristic peaks were identified at  $1,096\text{ cm}^{-1}$ , a sharp and intense peak, due to the asymmetric vibration of Si–O–Si and at  $948\text{ cm}^{-1}$ , attributed to the Si–O–H stretching vibrations. A small peak at  $1,625\text{ cm}^{-1}$  appears to be attributed to the hydroxyl group revealing the formation of silicon shell (Chang et al., 2012). For the functionalized (silanized) sample, the presence of a shoulder observed at  $1,710\text{ cm}^{-1}$  could be assigned to the carbonyl group C=O from the MPS (Figure 3C). Finally, a wide, broad band was observed between  $3,100$  and  $3,500\text{ cm}^{-1}$  corresponding to the NH bonds of a primary amide of the polyacrylamide formed, and the peak at  $1,635\text{ cm}^{-1}$  would correspond to the vibration of the C=O. The weak peaks at  $1,120$  and  $1,213\text{ cm}^{-1}$  correspond to C–N vibration. These results confirmed that the coating with acrylamide-based polymer was performed satisfactorily (Figure 3D).

The magnetic behavior of the synthesized material was studied by magnetization curves (VSM) at  $300\text{ K}$ . Figure 4 shows that all the curves present the same characteristics: the absence of hysteresis and coercivity, suggesting that all the samples are superparamagnetic. The saturation magnetization ( $M_s$ ) value obtained for magnetite was  $44.5\text{ emu g}^{-1}$  which drastically decreased to  $14.3$ ,  $8.3$ , and  $1.3\text{ emu g}^{-1}$  for  $\text{Fe}_3\text{O}_4@SiO_2$ ,  $\text{Fe}_3\text{O}_4@SiO_2\text{-MPS}$ , mag-MIP, respectively. This decrease in magnetization values can be attributed to the increase of the coating layers of non-magnetic materials on the magnetite and therefore, the size, but keeping the superparamagnetic nature (Pan et al., 2014; Uzuriaga-Sánchez et al., 2016).



## Development of the Electrochemical Sensor Modified With Mag-MIP

Square wave voltammetry (SWV) technique was used to detect amoxicillin in a phosphate buffer solution of pH 7.0 using a mag-MIP/CPE sensor under optimized experimental conditions. The best experimental values for the SWV parameters were: step =  $5\text{ mV}$ , amplitude =  $50\text{ mV}$  and frequency =  $15\text{ Hz}$ .

The response profile by SWV of mag-MIP/CPE and mag-NIP/CPE in the presence of  $1.0\text{ mmol L}^{-1}$  of amoxicillin at  $0.72\text{ V}$  vs. Ag/AgCl is shown in Figure 5. The remarkable difference between mag-MIP and mag-NIP sensors is revealed and could be attributed to the presence of the selective cavities in the mag-MIP which increased the sensitivity in the amoxicillin detection, this behavior is also outlined in literature by other authors (Montoya et al., 2015; Yang et al., 2020). The expected profile of the non-selective polymer (mag-NIP/CPE) and CPE (electrode carbon paste) was not satisfactory as compared to magnetic selective polymer (mag-MIP/CPE). This fact can be explained by the lack of selective pore toward the analyte on the surface of the mag-NIP/CPE and in the CPE.

## Effect of pH

The pH is one of the most significant factors that could affect the performance of the electrochemical process. In the amoxicillin molecule (**Scheme 2**) when  $\text{pH} < \text{pK}_{a1}$  (2.4), the molecule accepts a proton forming an ion with a positive charge, causing electrostatic repulsion on the electrode surface. In the situation where the  $\text{pK}_{a1}$  (2.4)  $< \text{pH} < \text{pK}_{a2}$  (7.4), the molecule is not charged or ionized. When  $\text{pK}_{a2}$  (7.4)  $< \text{pH} < \text{pK}_{a3}$  (9.6), the molecule loses a proton forming an ion with a negative charge. When  $\text{pH} > \text{pK}_{a3}$  (9.6), the amoxicillin loses two protons

forming an ion with two negative charges, forming a phenolic anion that cannot be oxidized (Zhao et al., 2019).

The effect of pH on the response of the sensor was evaluated, as shown in **Figure 6**. As can be observed in **Figure 6A**, the pH increases up to 7.0 in which the signal is the highest, so the adsorption is highly favored. Then, the current decreases at pH near 8.0 and 9.0 when the amoxicillin is deprotonated and the phenolic group oxidation diminishes.

**Figure 6B** shows the influence of pH in the peak potential value, revealing a linear relationship with a slope of  $-0.067 \text{ V pH}^{-1}$  that is value next to the theoretical Nernstian slope of  $-0.059 \text{ V pH}^{-1}$ . This indicates that the redox process in this sensor corresponds to a system where the same number of protons and electrons are involved (Zeinali et al., 2018; Wong et al., 2020).

The electrochemical mechanism is shown in **Scheme 3**, where the oxidation of the phenolic group present in the amoxicillin is adsorbed on the electrode surface.

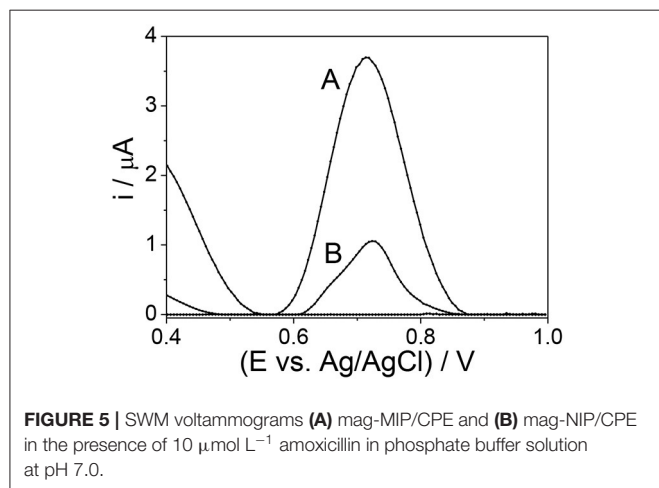
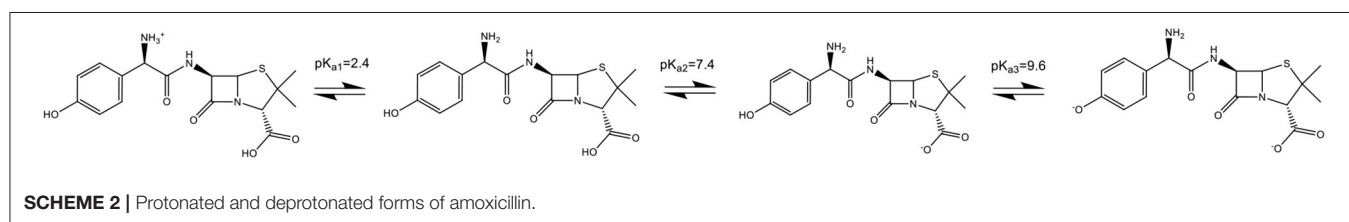


**FIGURE 5** | SWV voltammograms (A) mag-MIP/CPE and (B) mag-NIP/CPE in the presence of  $10 \mu\text{mol L}^{-1}$  amoxicillin in phosphate buffer solution at pH 7.0.

## Analytical Curve for Amoxicillin

To quantify amoxicillin in different matrices, the electrochemical analysis was made by the square wave voltammetry technique. **Figure 7** depicts a change in the magnitude of anodic peak current as a result of the addition of different amoxicillin concentrations. Under optimized conditions, the sensor had a response linear range from 2.5 to  $57 \mu\text{mol L}^{-1}$  amoxicillin ( $r^2 = 0.996$ ), with a limit of detection and limit of quantification of 0.75 and  $2.48 \mu\text{mol L}^{-1}$ , respectively.



**SCHEME 2** | Protonated and deprotonated forms of amoxicillin.

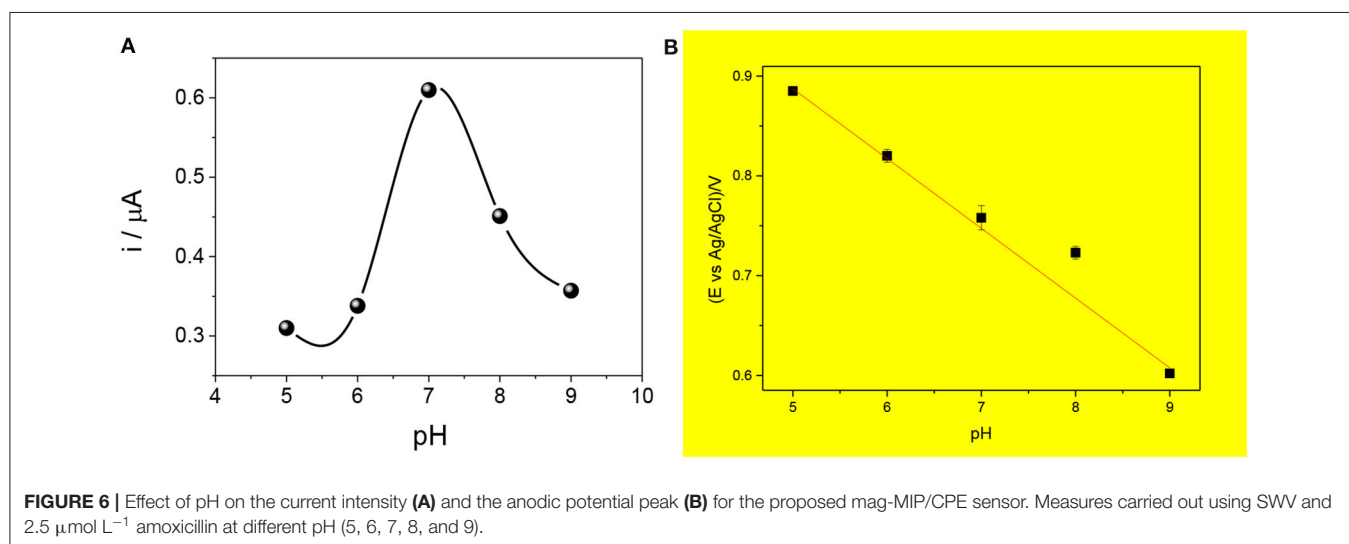
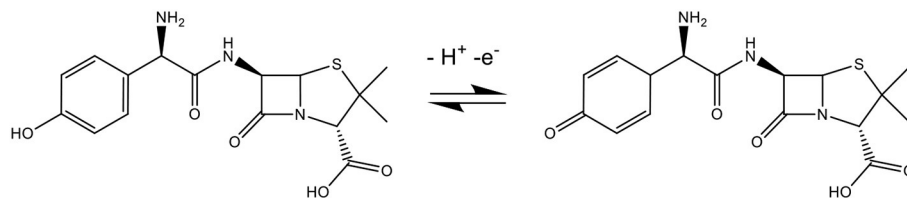


**FIGURE 6** | Effect of pH on the current intensity (A) and the anodic potential peak (B) for the proposed mag-MIP/CPE sensor. Measures carried out using SWV and  $2.5 \mu\text{mol L}^{-1}$  amoxicillin at different pH (5, 6, 7, 8, and 9).



**SCHEME 3** | Electrochemical oxidation mechanism of amoxicillin.

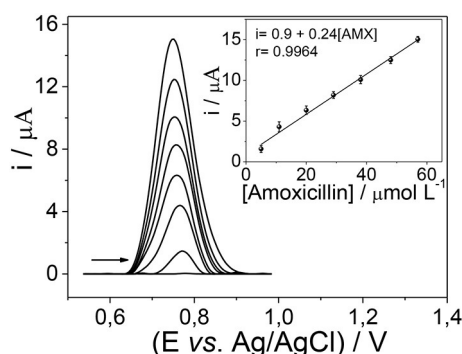


**FIGURE 7** | Electrochemical determination by SWV of amoxicillin using the mag-MIP/CPE sensor.

### Repeatability and Selectivity Studies

The repeatability was tested by 10 electrochemical measurements by SWV in presence of  $10 \mu\text{mol L}^{-1}$  of amoxicillin and was evaluated in terms of the relative standard deviation (RSD, Equation 1). The value obtained in this analysis was lower than 4%, indicating good repeatability and stability in the determination of this antibiotic using the proposed sensor.

$$\text{RSD} = \frac{S}{\bar{X}} \times 100 \quad (1)$$

In Equation (1),  $S$  represents the standard deviation and  $\bar{X}$  represents the average value.

The selectivity of the sensor was tested by comparing the SWV signal of the analyte against other chemicals heavily consumed in daily life (urea, caffeine, uric acid, ciprofloxacin, ascorbic acid, and sodium chloride). These studies were carried out in binary mixtures (analyte and other compounds) under optimized conditions in the concentration of  $5 \mu\text{mol L}^{-1}$ . The results showed no interference in the electrochemical signal of amoxicillin for triplicate experiments since in the presence of interfering compounds obtained error values lower than 5% to the sensor signal.

### Application of the Sensor in Skimmed Milk and River Water Samples

The mag-MIP/CPE sensor was applied to quantify amoxicillin in skimmed milk and river water samples, prepared as described in the experimental section. The analysis was performed in triplicate

**TABLE 1** | Recovery rates obtained from the use of the proposed mag-MIP/CPE sensor in the analysis of regional river water and skimmed milk samples spiked with known amoxicillin concentrations.

| Samples      | Place obtained                        | Added/mol L <sup>-1</sup> | Proposed method*/mol L <sup>-1</sup> | Recovery (%) |
|--------------|---------------------------------------|---------------------------|--------------------------------------|--------------|
| River water  | Gregório (São Paulo state—Brazil)     | $3.0 \times 10^{-6}$      | $(3.0 \pm 0.3) \times 10^{-6}$       | 100.3        |
|              |                                       | $8.0 \times 10^{-6}$      | $7.98 \times 10^{-6}$                | 98.8         |
|              |                                       | $3.0 \times 10^{-5}$      | $(3.0 \pm 0.2) \times 10^{-5}$       | 100.2        |
| Skimmed milk | Local market (São Paulo state—Brazil) | $3.0 \times 10^{-6}$      | $(2.9 \pm 0.2) \times 10^{-6}$       | 96.7         |
|              |                                       | $8.0 \times 10^{-6}$      | $7.9 \times 10^{-6}$                 | 97.5         |
|              |                                       | $3.0 \times 10^{-5}$      | $(2.9 \pm 0.3) \times 10^{-5}$       | 96.7         |

\*Standard deviation values corresponding to  $n = 3$ .

experiments and the number of amoxicillin present in the samples was calculated using the calibration curve. **Table 1** shows the recovery values obtained in the quantification of amoxicillin in these samples. The recovery values obtained were close to 100% using the SWV technique, showing good applicability of the proposed sensor in these matrices.

## CONCLUSION

The present work has reported on a simple and low-cost sensor for the quantification of amoxicillin in skimmed milk and river water samples. The use of mag-MIP contributed to the increase of the electrochemical signal from amoxicillin when compared with its non-impressed counterpart mag-NIP, as well as when the mag-MIP has a high surface area as compared with mag-NIP. The various factors influencing electrochemical determination such as pH, dose, contact time, and the concentration of an analyte, were optimized to get a maximum anodic current peak. The use of magnetic particles combined with MIP boosts its surface area which helps peak current increase. It is also easy to wash this material by using an external magnet instead of filtration.

The proposed sensor exhibited high stability, fast analysis time, good selectivity, and sensibility. Finally, the main advantages of the proposed method were the ability to renew the electrode surface by simple polishing allowing further analysis.

## DATA AVAILABILITY STATEMENT

The raw data supporting the conclusions of this article will be made available by the authors, without undue reservation.

## AUTHOR CONTRIBUTIONS

RL was responsible for experimental studies. SK and AW were responsible for experiments, revision of experiments, and initial redaction of the paper. MS was responsible for the submission, final revision, and financial support to this research. GP was responsible of the correction of the final version and for the financial support. All authors contributed to the article and approved the submitted version.

## REFERENCES

- Ansari, S. (2017). Application of magnetic molecularly imprinted polymer as a versatile and highly selective tool in food and environmental analysis: Recent developments and trends. *TrAC Trends Anal. Chem.* 90, 89–106. doi: 10.1016/j.trac.2017.03.001
- Cai, W., and Wan, J. (2007). Facile synthesis of superparamagnetic magnetite nanoparticles in liquid polyols. *J. Colloid Interface Sci.* 305, 366–370. doi: 10.1016/j.jcis.2006.10.023
- Carvalho, I. T., and Santos, L. (2016). Antibiotics in the aquatic environments: a review of the European scenario. *Environ. Int.* 94, 736–757. doi: 10.1016/j.envint.2016.06.025
- Chang, L., Chen, S., and Li, X. (2012). Synthesis and properties of core-shell magnetic molecular imprinted polymers. *Appl. Surf. Sci.* 258, 6660–6664. doi: 10.1016/j.apsusc.2012.03.102
- Christou, A., Agüera, A., Bayona, J. M., Cytryn, E., Fotopoulos, V., Lambropoulou, D., et al. (2017). The potential implications of reclaimed wastewater reuse for irrigation on the agricultural environment: the knowns and unknowns of the fate of antibiotics and antibiotic resistant bacteria and resistance genes – a review. *Water Res.* 123, 448–467. doi: 10.1016/j.watres.2017.07.004
- Ecker, L., Ochoa, T. J., Vargas, M., Del Valle, L. J., and Ruiz, J. (2013). Preferences of antibiotic use in children less than five in physicians working health centers of primary level in peri-urban areas of Lima, Peru. *Rev. Peru. Med. Exp. Salud Pública* 30, 181–189.
- Elizalde-Velázquez, A., Gómez-Oliván, L.M., Galar-Martínez, M., Islas-Flores, H., Dublán-García, O., and SanJuan-Reyes, N. (2016). “Amoxicillin in the aquatic environment, its fate and environmental risk,” in *Environmental Health Risk Hazard, Factors to Living Species*, eds M. L. Larramendy and S. Soloneski (Mexico City: IntechOpen). doi: 10.5772/62049
- Fouladgar, M., Hadjmohammadi, M. R., Khalilzadeh, M. A., Biparva, P., Teymoori, N., and Beitollah, H. (2011). Voltammetric determination of amoxicillin at the electrochemical sensor ferrocenedicarboxylic acid multi wall carbon nanotubes paste electrode. *Int. J. Electrochem. Sci.* 6, 1355–1366.
- Gao, M., Li, W., Dong, J., Zhang, Z., and Yang, B. (2011). Synthesis and characterization of superparamagnetic Fe<sub>3</sub>O<sub>4</sub>@SiO<sub>2</sub> core-shell composite nanoparticles. *World J. Condens. Matter Phys.* 1, 49–54. doi: 10.4236/wjcmp.2011.12008
- Hancu, G., Neacșu, A., Papp, L. A., and Ciurba, A. (2016). Simultaneous determination of amoxicillin and clavulanic acid in pharmaceutical preparations by capillary zone electrophoresis. *Brazilian J. Pharm. Sci.* 52, 281–286. doi: 10.1590/S1984-8250201600200006
- Jordán, D., González-Chávez, D., Laura, D., León Hilario, L. M., Montebancho, E., Gutarra, A., et al. (2018). Detection of magnetic moment in thin films with a home-made vibrating sample magnetometer. *J. Magn. Magn. Mater.* 456, 56–61. doi: 10.1016/j.jmmm.2018.01.088
- Karimi-Maleh, H., and Arotiba, O. A. (2020). Simultaneous determination of cholesterol, ascorbic acid and uric acid as three essential biological compounds at a carbon paste electrode modified with copper oxide decorated reduced graphene oxide nanocomposite and ionic liquid. *J. Colloid Interface Sci.* 560, 208–212. doi: 10.1016/j.jcis.2019.10.007

## FUNDING

This project was supported by FONDECYT-BM (grant #023-2019-FONDECYT-BM-IN.INV), FAPESP (grants #2019/00677-7 and #2014/50945-4), CNPq (grants #301728/2019-4, #408050/2018-7 and #465571/2014-0), and CAPES (PROJ. AUX/PE/PROEX N° 0674/2018). RL and GP received financial support from the OGI, Research Management Bureau (Project FC-F-6-2018).

- Karimi-Maleh, H., Karimi, F., Alizadeh, M., and Sanati, A. L. (2020a). Electrochemical sensors, a bright future in the fabrication of portable kits in analytical systems. *Chem. Rec.* 20, 682–692. doi: 10.1002/tcr.201900092
- Karimi-Maleh, H., Karimi, F., Orooji, Y., Mansouri, G., Razmjou, A., Aygun, A., et al. (2020b). A new nickel-based co-crystal complex electrocatalyst amplified by NiO doped Pt nanostructure hybrid; a highly sensitive approach for determination of cysteamine in the presence of serotonin. *Sci. Rep.* 10:11699. doi: 10.1038/s41598-020-68663-2
- Karimi-Maleh, H., Shojaei, A. F., Tabatabaeian, K., Karimi, F., Shakeri, S., and Moradi, R. (2016). Simultaneous determination of 6-mercaptopurine, 6-thioguanine and dasatinib as three important anticancer drugs using nanostructure voltammetric sensor employing Pt/MWCNTs and 1-butyl-3-methylimidazolium hexafluoro phosphate. *Biosens. Bioelectron.* 86, 879–884. doi: 10.1016/j.bios.2016.07.086
- Khan, S., Hussain, S., Wong, A., Foguel, M. V., Moreira Gonçalves, L., Pividori Gurgo, M. I., et al. (2018). Synthesis and characterization of magnetic-molecularly imprinted polymers for the HPLC-UV analysis of ametryn. *React. Funct. Polym.* 122, 175–182. doi: 10.1016/j.reactfunctpolym.2017.11.002
- Khan, S., Wong, A., Zanon, M. V. B., and Sotomayor, M. D. P. T. (2019). Electrochemical sensors based on biomimetic magnetic molecularly imprinted polymer for selective quantification of methyl green in environmental samples. *Mater. Sci. Eng. C* 103:109825. doi: 10.1016/j.msec.2019.109825
- Kishore, M., Jayaprakash, M., and Vijayabhaskarareddy, T. (2011). Spectrophotometric determination of capecitabine in pharmaceutical formulations. *Int. J. ChemTech Res.* 3, 63–69.
- Laurent, S., Forge, D., Port, M., Roch, A., Robic, C., Vander Elst, L., et al. (2008). Magnetic iron oxide nanoparticles: synthesis, stabilization, vectorization, physicochemical characterizations and biological applications. *Chem. Rev.* 108, 2064–2110. doi: 10.1021/cr068445e
- Lu, A. H., Salabas, E. L., and Schüth, F. (2007). Magnetic nanoparticles: synthesis, protection, functionalization, and application. *Angew. Chem. Int. Ed.* 46, 1222–1244. doi: 10.1002/anie.200602866
- Martínez, J. L. (2009). Environmental pollution by antibiotics and by antibiotic resistance determinants. *Environ. Pollut.* 157, 2893–2902. doi: 10.1016/j.envpol.2009.05.051
- Miège, C., Choubert, J. M., Ribeiro, L., Eusebe, M., and Coquery, M. (2009). Le devenir des résidus pharmaceutiques dans les stations d'épuration d'eaux usées. Une synthèse de la littérature. *TSM. Tech. Sci. Méthodes Génie Urbain Génie Rural*, 11, 75–94. doi: 10.1051/tsm/200911075
- Montoya, P., Mejía, S., Gonçalves, V. R., Torresi, S. I. C., De, and Calderón, J. A. (2015). Performance improvement of macroporous polypyrrole sensor for detection of ammonia by incorporation of magnetite nanoparticles. *Sensors Actuat. B Chem.* 213, 444–451. doi: 10.1016/j.snb.2015.02.118
- Pan, S. D., Shen, H. Y., Zhou, L. X., Chen, X. H., Zhao, Y. G., Cai, M. Q., et al. (2014). Controlled synthesis of pentachlorophenol-imprinted polymers on the surface of magnetic graphene oxide for highly selective adsorption. *J. Mater. Chem. A* 2, 15345–15356. doi: 10.1039/c4ta02600d
- Pires de Abreu, L., Mas Ortiz, R. A., Calafatti de Castro, S., and Pedrazzoli, J. (2003). HPLC determination of amoxicillin comparative bioavailability in healthy volunteers after a single dose administration. *J. Pharm. Pharm. Sci.* 6, 223–230.



- Pizan-Aquino, C., Wong, A., Avilés-Félix, L., Khan, S., Picasso, G., and Sotomayor, M. D. P. T. (2020). Evaluation of the performance of selective M-MIP for tetracycline using electrochemical and HPLC-UV method. *Mater. Chem. Phys.* 245:122777. doi: 10.1016/j.matchemphys.2020.122777
- Stöber, W., Fink, A., and Bohn, E. (1968). Controlled growth of monodisperse silica spheres in the micron size range. *J. Colloid Interface Sci.* 26, 62–69. doi: 10.1016/0021-9797(68)90272-5
- Uzuriaga-Sánchez, R. J., Khan, S., Wong, A., Picasso, G., Pividori, M. I., and Sotomayor, M. D. P. T. (2016). Magnetically separable polymer (Mag-MIP) for selective analysis of biotin in food samples. *Food Chem.* 190, 460–467. doi: 10.1016/j.FOODCHEM.2015.05.129
- Vega-Chacón, J., Picasso, G., Avilés-Félix, L., and Jafelicci, M. (2016). Influence of synthesis experimental parameters on the formation of magnetite nanoparticles prepared by polyol method. *Adv. Nat. Sci. Nanosci. Nanotechnol.* 7:015014. doi: 10.1088/2043-6262/7/1/015014
- Verlicchi, P., Galletti, A., Petrovic, M., and Barceló, D. (2010). Hospital effluents as a source of emerging pollutants: an overview of micropollutants and sustainable treatment options. *J. Hydrol.* 389, 416–428. doi: 10.1016/j.jhydrol.2010.06.005
- Wong, A., Santos, A. M., Cincotto, F. H., Moraes, F. C., Fatibello-Filho, O., and Sotomayor, M. D. P. T. (2020). A new electrochemical platform based on low cost nanomaterials for sensitive detection of the amoxicillin antibiotic in different matrices. *Talanta* 206:120252. doi: 10.1016/j.talanta.2019.120252
- Wong, A., Scontri, M., Materon, E. M., Lanza, M. R. V., and Sotomayor, M. D. P. T. (2015). Development and application of an electrochemical sensor modified with multi-walled carbon nanotubes and graphene oxide for the sensitive and selective detection of tetracycline. *J. Electroanal. Chem.* 757, 250–257. doi: 10.1016/j.jelechem.2015.10.001
- World Health Organization (2019). *New report calls for urgent action to avert antimicrobial resistance crisis.* *Jt. News Release.* Available online at: <https://www.who.int/news-room/detail/29-04-2019-new-report-calls-for-urgent-action-to-avert-antimicrobial-resistance-crisis#:~:text=By%2030%2C%20antimicrobial%20resistance%20could,die%20from%20multidrug-resistant%20tuberculosis> (accessed October 2, 2020).
- Yang, Y., Yan, W., Guo, C., Zhang, J., Yu, L., Zhang, G., et al. (2020). Magnetic molecularly imprinted electrochemical sensors: a review. *Anal. Chim. Acta* 1106, 1–21. doi: 10.1016/j.aca.2020.01.044
- Zeinali, S., Khoshafar, H., Rezaei, M., and Bagheri, H. (2018). Fabrication of a selective and sensitive electrochemical sensor modified with magnetic molecularly imprinted polymer for amoxicillin. *Anal. Bioanal. Chem. Res.* 5, 195–204. doi: 10.22036/abcr.2018.104434.1174
- Zhao, J., Sun, Y., Wu, F., Shi, M., Liu, X., and Meca, G. (2019). Oxidative degradation of amoxicillin in aqueous solution by thermally activated persulfate. *J. Chem.* 2019:2505823. doi: 10.1155/2019/2505823

**Conflict of Interest:** The authors declare that the research was conducted in the absence of any commercial or financial relationships that could be construed as a potential conflict of interest.

Copyright © 2021 López, Khan, Wong, Sotomayor and Picasso. This is an open-access article distributed under the terms of the Creative Commons Attribution License (CC BY). The use, distribution or reproduction in other forums is permitted, provided the original author(s) and the copyright owner(s) are credited and that the original publication in this journal is cited, in accordance with accepted academic practice. No use, distribution or reproduction is permitted which does not comply with these terms.